

TEM and XRD investigation of Fe₂O₃-Al₂O₃ system

Camelia OPREA* and Viorel IONESCU

Ovidius University of Constanta, Department of Physics, 124 Mamaia Blvd, 900527, Romania

Abstract. A series of Fe₂O₃-Al₂O₃ mixed systems with composition ranging from 1 to 9% of Al₂O₃ were prepared by a traditional chemical method and examined for structural characteristics. XRD spectra and SAED patterns obtained from TEM investigations showed the presence of α -Al₂O₃ and α -Fe₂O₃ phases. The mean grain size of the crystalline aggregates in the system was calculated from BF-TEM images using the lognormal curve and verified with the Sherrer's formula applied on XRD diagrams, being established in the domain of 7-9 nm.

Keywords: oxidic system, BF-TEM, SAED, XRD

1. Introduction

Nanoparticles of α -Fe₂O₃, in its different phases, are being currently explored for their diverse range of applications such as magnetic storage media, environment protection, sensors, catalysis, clinical diagnosis and treatment etc. The attention which is being focused on their synthesis and characterization is well-deserved as they have the capability to exhibit certain superior properties as compared to bulk. In particular, superparamagnetic (SPM) nanoparticles of iron oxide are being used in biotechnology and biomedicine, as contrast agents in magnetic resonance imaging (MRI), as drug carriers for magnetically guided drug delivery, biosensors etc [1-3].

The oxidic systems including α -Al₂O₃ and α -Fe₂O₃ have been frequently investigated because of their importance in various environmental systems (soils and sediments) and industrial processes (bauxite mining, production of various ceramics).

Polli et al. [4] postulated, that the phase γ -(Al, Fe)₂O₃ directly transforms to α -(Al, Fe)₂O₃ solid solution without the prior nucleation of ferric oxide seeds. Bye and Simpkin [5] reported, that enhanced formation of α -(Al, Fe)₂O₃ could arise from segregation of Fe-rich clusters within γ -(Al, Fe)₂O₃ matrix, which could nucleate α -Al₂O₃ at much lower temperatures and acts as seeds for α -Al₂O₃.

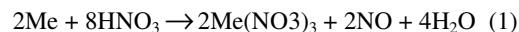
Vapor-grown carbon nanofibers (CNFs), with many applications developed for field emission

display, electrodes and reinforcement of materials were synthesized from a Fe₂O₃-Al₂O₃ composite mixture under C₂H₄ and H₂ flow at 600°C [6].

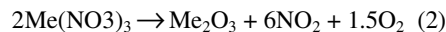
The purpose of this paper is to obtain chemically some Fe₂O₃-Al₂O₃ mixed systems including solid solutions with the general formula α -(Al_xFe_{1-x})₂O₃, 0 ≤ x ≤ 1, and to present some details about the grains dimension with the help of transmission microscopy and x-ray diffraction.

2. Experimental

First step for the production of Fe₂O₃-Al₂O₃ mixed system was the dissolution of Me (Me=Fe, Al) in nitric acid providing an acid solution of Me(NO₃)₃ by reaction:



Next, it was established a thermal decomposition of the combined metal nitrate solution and promoter acid nitrate solution by calcinations in the porcelain capsule at open flame for about 6-7 hours. The reaction for the pure decomposition of Me(NO₃)₃ was:



Using well established quantities of the metallic nitrates, it was obtained systems of amorphous solid solutions, with the following concentrations:

Samples concentration (%mol)

α - Al ₂ O ₃	α - Fe ₂ O ₃
98	2
96	4
94	6

XRD analysis was carried out with a TUR-M62 X-ray spectrometer.

The low-angle X-ray diffraction analyses were performed to establish the presence of the crystalline phases in the system and to calculate the average crystalline size of the particles, using Sherrer's formula. The microstructure of the Fe₂O₃-Al₂O₃ mixed oxidic systems was analysed by transmission electron microscopy (TEM).

TEM measurements were made using a higher resolution electron microscope, Philips CM 120, operating at an accelerating voltage of 100 kV and capable of a point-to point resolution of 2 Å.

With the Bright – Field Transmission Electron Microscopy (BF-TEM) image, we studied the granular structure of the film, and we plotted a grain size distribution for the probes.

3. Results and discussions

From the BF-TEM images of the Fe₂O₃ -Al₂O₃ samples shown in fig.1.(a), fig.2.(a) and fig.3(a), we can say that in the probes investigated were formed some crystalline conglomerates with the maximum diameters of few dozen nanometers.

The diffraction rings presented in the pattern from fig.1.(b) for the system probe with the lowest Al₂O₃ concentration (1%) are corresponding to the interplanar distances of 0.264 nm, 0.219 nm, 0.169 nm, and 0.144 nm, which fits well with the distances of the (104), (113), and (116) diffraction planes for the trigonal phase of hematite α - Fe₂O₃.

The SAED patterns from fig.2.b and fig.3.b. indicated the presence of both crystalline phases for Fe₂O₃ and Al₂O₃ in the systems investigated.

The size distributions of the crystalline formations identified and showed by different colours in fig.1.a and 2.a and obtained from the diameter measurements of a few dozen granules are

plotted.4. The distribution of grain sizes, as measured from BF-TEM image, was fitted to the lognormal curve. The mean aggregates size, D_m, was found to be of about 6 nm for the 99%Fe₂O₃ - 1%Al₂O₃ sample, and 11 nm for the other two samples investigated.

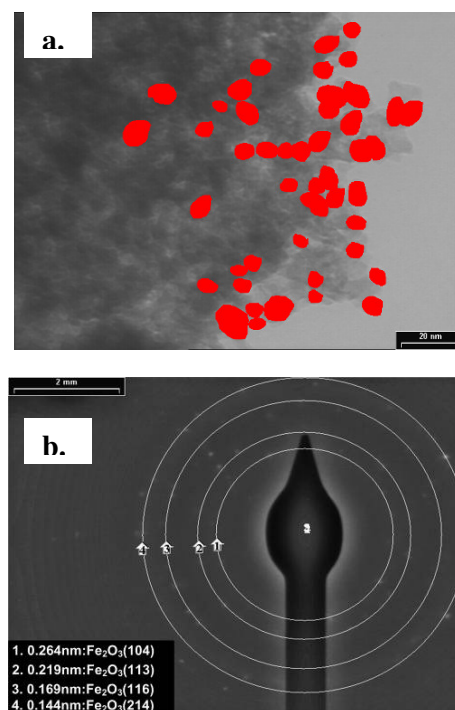


Fig. 1. BF-TEM image(a) and typical SAED pattern(b) of 99%Fe₂O₃ -1%Al₂O₃ system sample .

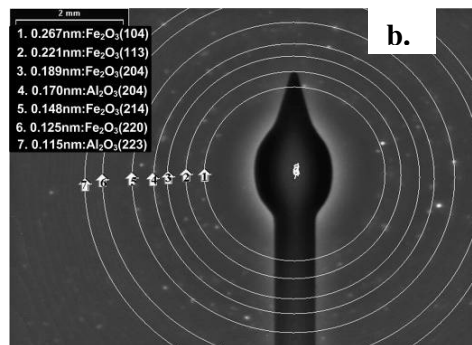
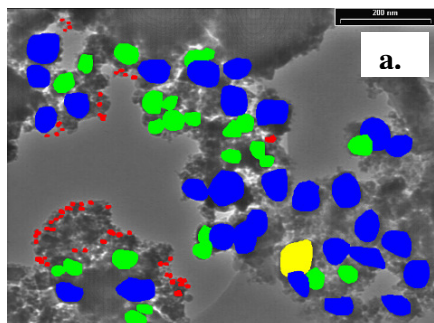


Fig. 3 BF-TEM image(a) and typical SAED pattern(b) of 91%Fe₂O₃ -9%Al₂O₃ system sample.

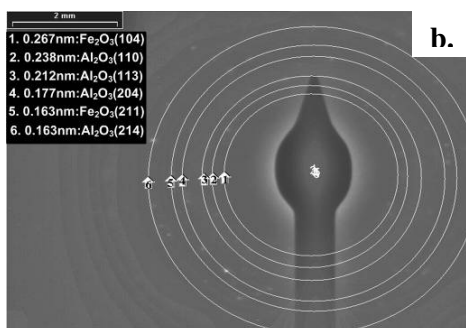
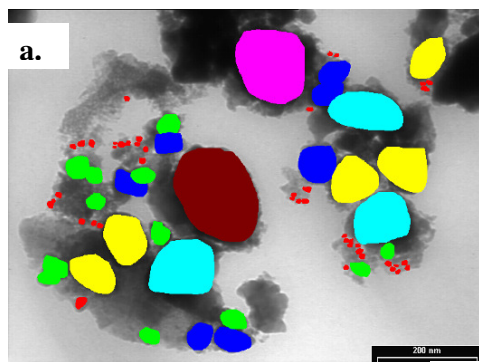
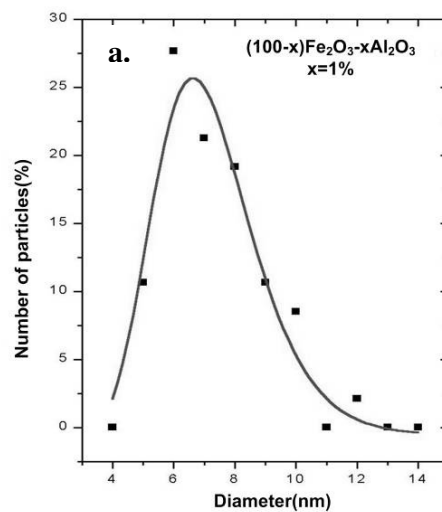


Fig. 2. BF-TEM image(a) and typical SAED pattern(b) of 97%Fe₂O₃ -3%Al₂O₃ system sample .



b.



From fig.5. we could observe that the α -Fe₂O₃ crystalline peaks of hematite indexed using the crystallographic database of Blake R.L. et al.[7] are very clear and predominant in the spectrum.

At the higher concentration of the Al₂O₃ component in the system, we observed a strong perturbation of the crystalline phase of Fe₂O₃ and the existence of some clear specific peaks for α -Al₂O₃, indexed using the crystallographic database of Lewis J. et al. [8], and corresponding to the diffraction planes of (110), (024), (300)(see fig.6).

The aluminium oxide has the tendency to form an amorphous phase more easily than the iron oxide, and at the concentration of 9% for Al₂O₃, the amorphous phase is predominant in the spectra showed in fig.7; we still could see some Al₂O₃ characteristic peaks in this diagram, corresponding to the diffraction planes of (202), (116) and (300).

From the XRD spectra we could observe the existence of some unidentified peaks, which could be associated with the presence of other (Al_xFe_{1-x})₂O₃ solid solutions in the oxidic system.

A. Ladavos and al.[9] prepared a series of Fe₂O₃-Al₂O₃ mixed oxidic solids by a sol-gel method, varying the Fe₂O₃ composition from 0 to 100%, and showed from XRD measurements the presence of α -Al₂O₃ and hematite phases.

Ignoring the microstraining effect (which affects the XRD peak width), as a first-order approximation, the average crystalline size can be estimated by the Debye – Scherrer formula [10]:

$$D = \frac{K\lambda}{\beta \cos \theta} \quad (3)$$

where K is a constant ($K = 0.91$), D is the mean crystalline dimension normal to diffracting planes, λ is the X-ray wavelength ($\lambda = 0.15406$ nm in our case), β in radian is the peak width at half-maximum height, and θ is the Bragg's angle. The calculated mean grain size D of crystallites for Fe₂O₃(104) peak from the XRD diffractogram showed in fig.5 and for Al₂O₃(110) peak presented in fig.6 was about 7nm and 9nm, respectively.

4. Conclusions

SAED patterns accomplished on the Fe₂O₃ - Al₂O₃ oxidic compounds revealed the presence of Al₂O₃ and Fe₂O₃ crystalline phases. The sample of 97%Fe₂O₃ -3%Al₂O₃ presented the strongest peaks for an XRD spectrum, some specific diffraction planes for both crystalline phases: corundum(Al₂O₃) and hematite(Fe₂O₃) being clearly revealed.

The mean grain size of the crystallites, resulting from Sherrer's formula calculation are varying in the domain of a 7-9nm in the oxidic systems.

5. References

*Email: coprea@univ-ovidius.ro

- [1]. T.P. Raming, A.J.A. Winnubst, C.M. Kats and P.A. Philipse, *Journal of Colloid and Interface Science*, **249**, 346–350 (2002).
- [2]. Liang-Shu Zhong, Jin-Song Hu, Han-Pu Liang, An-Min Cao, Wei-Guo Song and Li-Jun Wan, *Advanced Materials* **18**, 2426–2431 (2006).
- [3]. P. Chauhan, S. Annapoorni and S.K. Trikha, *Thin Solid Films* **346**, 266–268 (1999).
- [4]. A. D.Polli, F. E.Lange, C. G.Levi and J.Mayer, *J. Am.Ceram. Soc.* **79**, 55 (1996).
- [5]. G. C.Bye and G. T.Simpkin, *J. Am. Ceram. Soc.* **57**, 367 (1974).
- [6]. M. Maruyama, T.Fukasawa, S. Suenaga and Y. Goto, *Journal of the European Ceramic Society* **24**, 463-468 (2004).
- [7]. R.L.Blake, R.E.Hessevick, T.Zoltai and L.W Finger, *American Mineralogist* **51**, 123-129 (1966).
- [8]. J.Lewis, D.Schwartzbach and H.D.Flack, *Acta Crystallographica* **A38**, 733-739 (1982).
- [9]. A.Ladavos and T.Bakas, *Reaction Kinetics and Catalysis Letters*, **73**, 223-228 (2001).
- [10]. M.V. Zdujic, O.B. Milosevic and L. Karanovic, *Mater. Lett.* **13**, 125 (1992).